

Synthesis and Characterization of Undoped and Mo Doped Ferrihydrite Nanoparticles

A Project report submitted

in Partial Fulfillment of the Requirements

for the degree of

MASTER OF SCIENCE

in

PHYSICS

by

Pratibha Garg

(Roll No: 301304007)



SCHOOL OF PHYSICS AND MATERIALS SCIENCE

THAPAR UNIVERSITY

PATIALA-147004

INDIA

July 2015

***DEDICATED TO
MY LOVING
ONES***

Certificate

This is to certify that the project report entitled “Synthesis and Characterization of Undoped and Mo Doped Ferrihydrate Nanoparticles” submitted by Ms. Pratibha Garg is in partial fulfillment for degree of Master of Science in Physics in this University. This work has been done under my supervision. She has not submitted this material for credit towards any other degree at this or any other University.



(Dr. S. D. Tiwari)

Assistant Professor

School of Physics and Materials Science

Thapar University, Patiala

Countersigned by



Dr. Manoj K. Sharma

Head

School of Physics and Materials Science

Thapar University, Patiala



Dr. S.S. Bhatia

Dean of Academic Affairs

Thapar University, Patiala

Declaration

I hereby declare that the project report entitled “Synthesis and Characterization of Undoped and Mo Doped Ferrihydrite Nanoparticles” is the work carried out by me under the supervision of Dr. S. D. Tiwari. I have not submitted this work anywhere else for the award of any degree.



Pratibha Garg

Acknowledgement

First of all, I express my sincere gratitude to my supervisor Dr. S. D. Tiwari for his guidance and encouragement throughout the course of this work.

I would like to thank Dr. Manoj K. Sharma, Head SPMS, for his constant support. I thank Dr. B. N. Chudasama for characterizing my samples by TGA/DSC.

I express words of thanks from the bottom of my heart to Ph. D. scholars Ms. Chandni Rana and Ms. Anu Gupta for their cordial support and valuable information which helped me in completing this task through various stages.

Lastly, I thank almighty, my parents and my friends for their constant encouragement without which this assignment would not be possible.

Pratibha Garg

Abstract

Undoped and Mo doped two lines ferrihydrite nanoparticles are prepared by chemical route. The samples are characterized by x-ray diffractometer, transmission electron microscope, thermo-gravimetric analyzer, differential scanning calorimeter and vibrating sample magnetometer. The average crystallite size and particle size are found to be about 2 nm for both systems. The samples are found to decompose on heating at higher temperatures. The prepared nanoparticles of undoped and Mo doped ferrihydrite are found to be antiferromagnetic at room temperature.

Contents

Acknowledgement.....	v
Abstract.....	vi
Contents.....	vii
List of Figures.....	viii
Chapter-1 Introduction	1
1.1 Magnetic Materials.....	1
1.2 Superparamagnetism.....	5
1.3 Literature Review.....	5
Chapter-2 Experimental Details	8
2.1 Synthesis.....	8
2.2 Characterization Techniques.....	8
Chapter-3 Results and Discussions	13
3.1 Structural Characterization	13
3.2 Thermal Analysis	16
3.3 Magnetization	17
Chapter-4 Conclusion	19
References.....	20

List of Figures

Fig. 1.1: Arrangement of magnetic moments in ferromagnetic materials.

Fig. 1.2: Arrangement of magnetic moments in diamagnetic materials.

Fig. 1.3: Arrangement of magnetic moments in paramagnetic materials.

Fig. 1.4: Arrangement of spins in antiferromagnetic materials.

Fig. 1.5: Arrangement of spins in ferrimagnetic materials.

Fig. 2.1: Diffraction of X-Ray beam.

Fig. 2.2: Transmission Electron Microscope.

Fig. 2.3: Thermogravimetric analyzer.

Fig. 2.4: Differential scanning calorimeter.

Fig. 2.5: Vibrating Sample Magnetometer.

Fig. 3.1: X-ray diffraction pattern of undoped ferrihydrite nanoparticles.

Fig. 3.2: X-ray diffraction pattern of Mo doped ferrihydrite nanoparticles.

Fig. 3.3: TEM micrograph of undoped ferrihydrite nanoparticles.

Fig. 3.4: TEM micrograph of Mo doped ferrihydrite nanoparticles.

Fig. 3.5: TGA-DSC curves for undoped ferrihydrite nanoparticles.

Fig. 3.6: TGA-DSC curves for Mo doped ferrihydrite nanoparticles.

Fig. 3.7: M-B loop for undoped and Mo doped ferrihydrite nanoparticles at room temperature.

CHAPTER 1

INTRODUCTION

Physical properties of bulk materials do not depend on size of particles. However if particle size decreases to nanometer range then behavior of such systems are seen to strongly depend on size of particles. In other words, nanoparticles are expected to show interesting and unusual physical and chemical behaviors, unobservable in bulk materials [1, 2]. These new behaviors are mainly due to small size of crystals and large surface area.

Among nanoparticles of different materials, those of magnetic materials are relatively more attracting because of interesting observations and useful applications such as in catalysis, biomedicine, nano fluids, data storage etc. [3].

1.1 MAGNETIC MATERIALS

Orbital motion and spin of electron in an atom or ion are responsible for the origin of atomic or ionic magnetic moment. On the basis of behavior exhibited by materials in external magnetic field, all materials can be classified into following main categories [4-9].

1.1.1 FERROMAGNETIC MATERIALS

Ferromagnetic materials have large and positive magnetic susceptibilities. These materials are strongly attracted by an external magnetic field. Ferromagnetic materials are able to retain their magnetization even after the magnetic field is removed. These materials are divided into small microscopic regions, called magnetic domains, to minimize their internal energy. In each domain, magnetic moments are aligned in same direction. In absence of any external applied magnetic field, all domains are randomly oriented. This situation gives rise to zero value for the magnetization. When an external magnetic field is applied, the domains start aligning themselves along applied field direction. Examples of ferromagnetic materials are iron, nickel, cobalt etc.

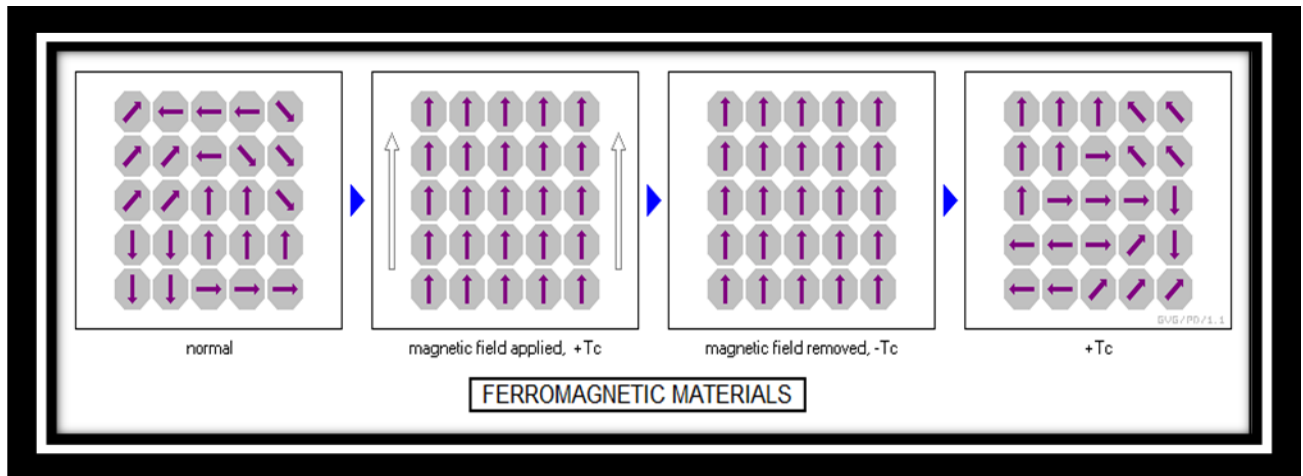


Fig. 1.1: Arrangement of magnetic moments in ferromagnetic materials [9].

1.1.2 DIAMAGNETIC MATERIALS

Diamagnetic materials do not have any unpaired electrons. These materials have weak and negative magnetic susceptibility. Diamagnetic materials are slightly repelled by an external magnetic field. The diamagnetic material loses its magnetization when the applied is removed.

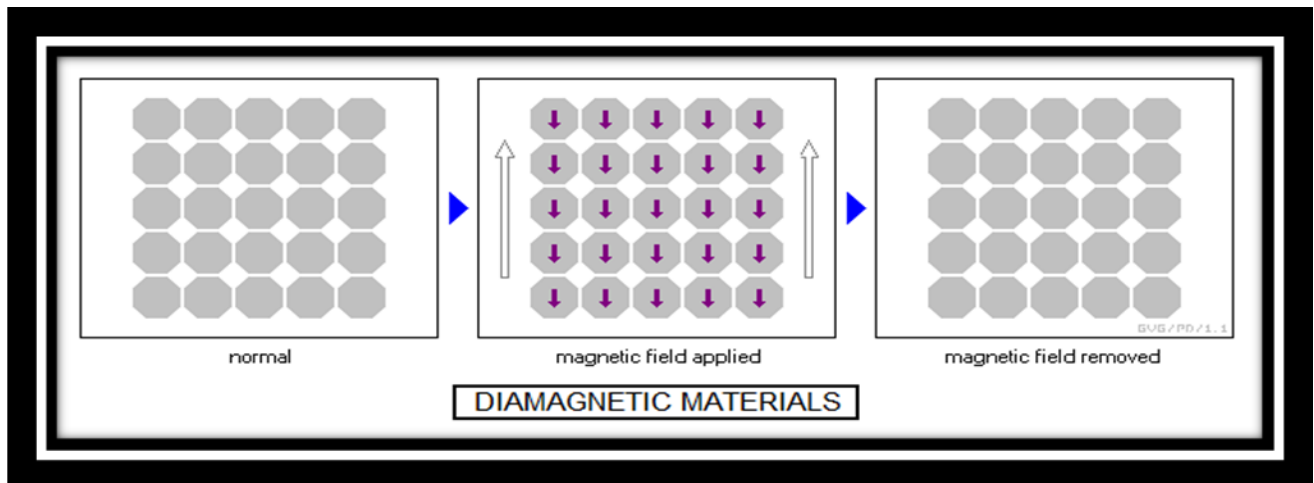


Fig. 1.2: Arrangement of magnetic moments in diamagnetic materials [9].

1.1.3 PARAMAGNETIC MATERIALS

Paramagnetic materials consist of non interacting unpaired electrons. When magnetic field is applied to these materials the magnetic moments try to align themselves along the field direction. These materials have small but positive magnetic susceptibility. These are slightly attracted by the magnetic field. Paramagnetic material losses its magnetization when the external magnetic field is removed.

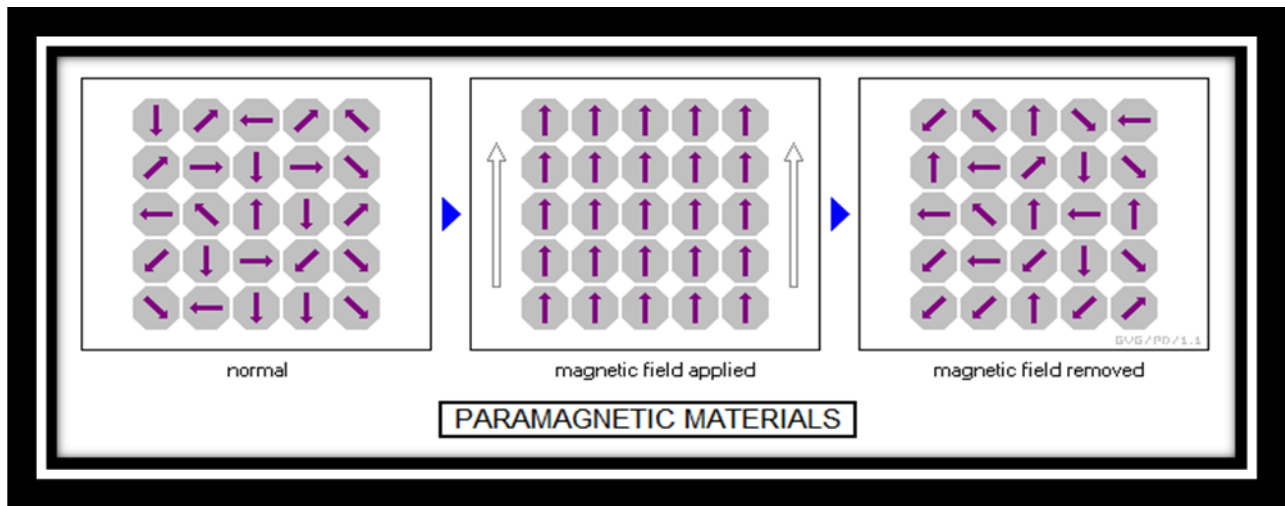


Fig. 1.3: Arrangement of magnetic moments in paramagnetic materials [9].

1.1.4 ANTIFERROMAGNETIC MATERIALS

In antiferromagnetic materials, the neighboring spins are arranged antiparallel to each other. Due to this, the material possesses zero net magnetization. Above a critical temperature, known as the Neel temperature T_N , the antiferromagnetic ordering breaks and the material becomes paramagnetic.

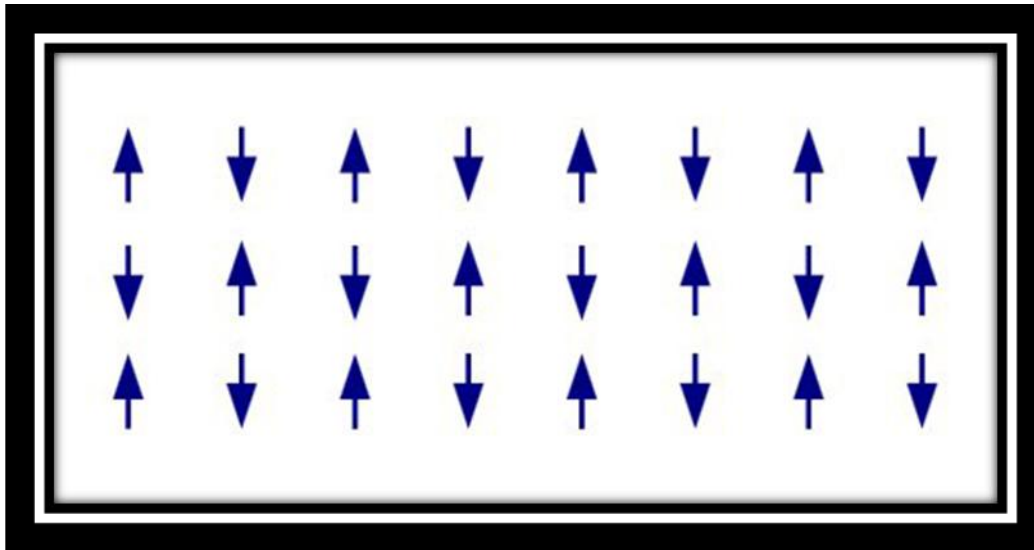


Fig. 1.4: Arrangement of spins in antiferromagnetic materials [10].

1.1.5 FERRIMAGNETIC MATERIALS

In ferrimagnetic materials, the neighboring spins are arranged in opposite directions. But the magnitudes of neighboring spins are not equal to each other as in the case of antiferromagnetic materials. Due to this, the ferromagnetic materials possess non-zero magnetization. Above a critical temperature, the ferrimagnetic material becomes paramagnetic.

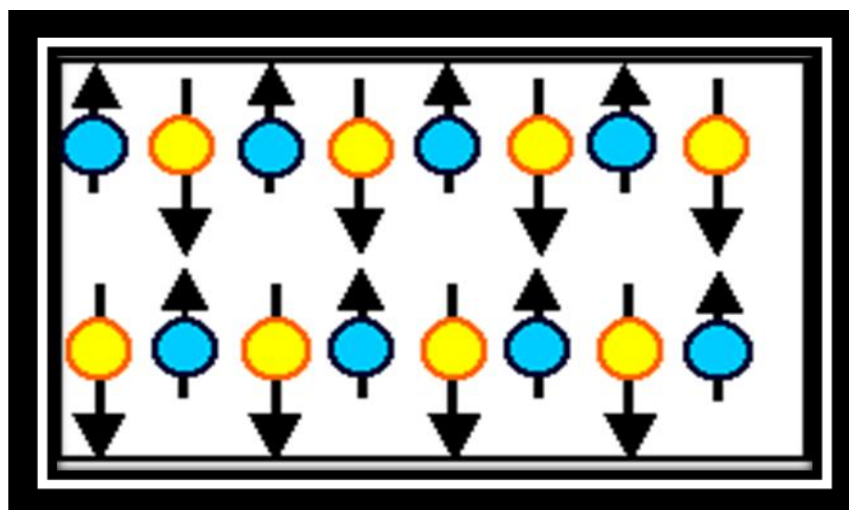


Fig. 1.5: Arrangement of spins in ferrimagnetic materials [11].

1.2 SUPERPARAMAGNETISM

Superparamagnetism is exhibited by small particles of ferro and ferrimagnetic materials. In absence of any external applied magnetic field the magnetization vector of a ferromagnetic material is directed along the easy axis. The direction of magnetization vector can be rotated by the application of an external magnetic field. The energy associated with the orientation of magnetization vector is known as the anisotropy energy. This energy is directly proportional to the volume of particles. If the thermal energy becomes larger than the anisotropy energy then the magnetization vector will be no longer fixed in direction. This situation is termed as superparamagnetism. The phenomenon of superparamagnetism is also exhibited by small particles of antiferromagnetic materials. For antiferromagnetic materials, the anisotropy energy signifies the energy required to change the direction of spins by 180 degrees [12].

1.3 LITERATURE REVIEW

Drits et al. (1993): Structure of 6-line and 2-line ferrihydrite nanoparticles is studied in detail. It is shown that ferrihydrite consists of three components (i) Ferrihydrite having no defect consisting of anionic ABACA (ii) defective ferrihydrite which consists of Ac_1Bc_2A and Ab_1Cb_2A structural fragments that alternate completely at random (iii) ultra dispersed hematite [13].

Zhao et al. (1994): Ferrihydrite nanoparticles were prepared by precipitation method. Analysis of X-Ray absorption fine structures shows the presence of lower coordination sites in the material. Sites are tetrahedral and are believed to be at the surface. Since impurity ions are present in the precipitation solution, these sites may absorb the impurity anions, thereby blocking the crystal growth sites and inhibiting the formation of hematite [14].

Jambor et al. (1998): X-Ray spectroscopic studies have indicated that there is a similarity in ferrihydrite structure and the FeOOH-type minerals such as, goethite and akaganeite. It was estimated that the iron in ferrihydrite is octahedrally coordinated, but it has also been proposed

that the octahedral coordination represents only the inner structure, and much of the surface of the ferrihydrite has iron in tetrahedral coordination [15].

Seehra et al. (2000): Two lines ferrihydrite nanoparticles were synthesized. The peak that is identified by the comparison of the neutron scattering and x-ray diffraction patterns is (002) peak. The intensity of this peak, when measured between 10 and 450 K, decreases linearly with temperature until 350 K, and become temperature independent above 350 K. This temperature is considered to be the ordering temperature of the inner spins of the nanoparticles [16].

Punnoose et al. (2004): Magnetic behavior of undoped and three doped samples of two lines ferrihydrite nanoparticles were studied and compared in details. It was found that Mo and Ir preferentially substitute for the surface Fe^{3+} ions and Ni substitutes for Fe^{3+} ions throughout the nanoparticles [17].

Michel et al. (2007): It was recognized that the 2-line and 6-line forms are the two types of ferrihydrite. There are no significant differences in these two forms and differences in the diffraction patterns can be interpreted by variable size of the coherent scattering domains. The average crystallite sizes found from the PDF analysis are same as observed by high-resolution transmission electron microscopy [18].

Carta et al. (2009): They prepared and characterized the two main forms of ferrihydrite that are 2-lines and 6-lines, on the basis of the number of reflections observed in the X-ray diffraction pattern. It was reported that the structure of two forms is quite similar and the small differences between the 2-lines and 6-lines ferrihydrite samples are mainly caused by the different weight of the magnetic spins located on the particle surface [19].

Dyer et al. (2010): The ferrihydrite particles were prepared using crystallization process. It was concluded that when silicate species are adsorbed on the surface of ferrihydrite, then it speeds up the polymerization process sites. It was also reported that the precipitation of silica proceeds more fastly in ferric nitrate media, than in ferric sulfate [20].

Das et al. (2011): It was suggested that two-line ferrihydrite transforms to hematite through a two-stage crystallization process, where goethite becomes the intermediate step. It was also reported that the findings of this study can be used to estimate rates of crystallization of pure two-line ferrihydrite over the broad range of temperatures [21].

Chandni et al. (2015): It was reported that the magnetization of two lines ferrihydrite nanoparticles can be fitted quite well to the modified Langevin function only if a distribution in particle magnetic moment is considered. This distribution of particle magnetic moment arises mainly due to distribution in particle shape and size [22].

CHAPTER 2

EXPERIMENTAL DETAILS

2.1 SYNTHESIS

In this work nanoparticles of ferrihydrite are synthesized by a chemical route [17]. The nanoparticles are prepared by reaction between ferric nitrate and sodium hydroxide aqueous solutions. For this sodium hydroxide aqueous solution is added drop wise to an aqueous solution of ferric nitrate with constant stirring until pH of the system reaches to 7.5. The resulting precipitate is filtered and washed several times with distilled water. The precipitate is dried at 50 °C and ground to get a powder sample.

Nanoparticles of ferrihydrite doped with 10 atomic percent Mo are synthesized by chemical route. For this, sodium hydroxide solution is added drop wise into an aqueous solution containing Fe³⁺ and Mo²⁺ ions in appropriate ratio until pH of the system reaches to 7.5. The resulting precipitate is filtered and washed several times with distilled water. The precipitate is dried at 50 °C and ground to get a powder sample.

2.2 CHARACTERISATION TECHNIQUES

2.2.1 X-RAY DIFFERATION

X-ray powder diffraction is a technique used for phase identification of crystalline materials. This also provides information of unit cell dimensions. This method is popularly used for structural characterization of unknown materials. In this technique, a monochromatic beam of x-rays is allowed to fall on a powder sample. The intensity of diffracted beam is found to be maximum when

$$2 d \sin \theta = n \lambda$$

where d is interplaner spacing and λ is the wavelength of x-ray used. Here $n = 1, 2, \dots$. This relation is known as Bragg's law [4].

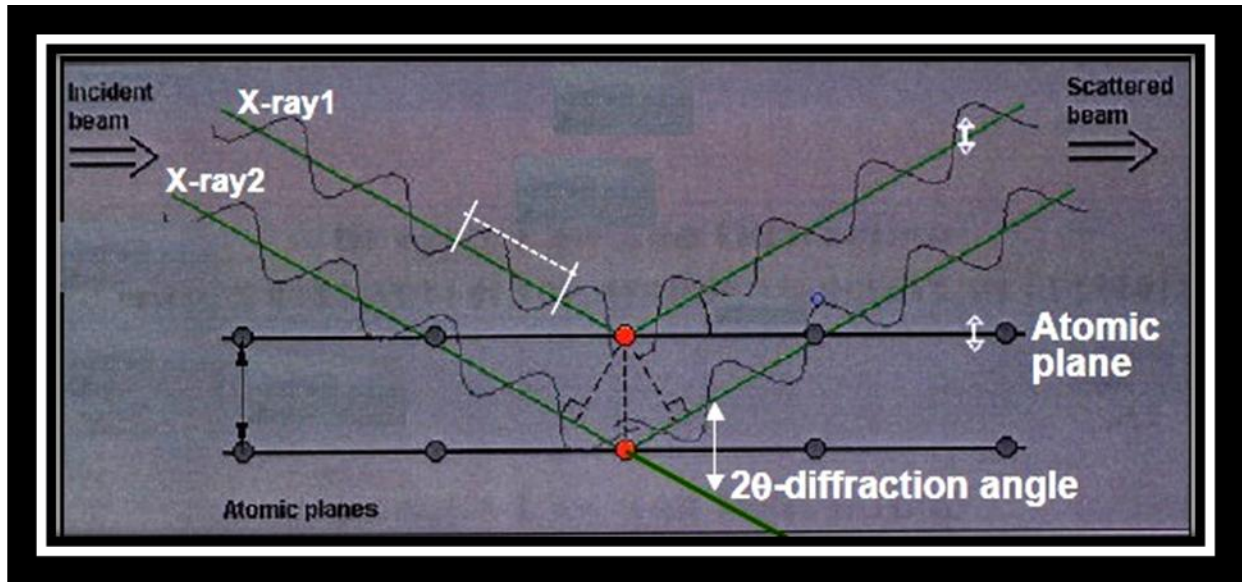


Fig. 2.1: Diffraction of X-Ray beam [23].

2.2.2 TRANSMISSION ELECTRON MICROSCOPE

In transmission electron microscope, an energetic beam of electrons is incident on a thin specimen [24]. The transmitted beam is used to get a magnified image of specimen. We can also study the diffraction of electrons by the sample for phase identification. In this microscope, magnetic lenses, which are current carrying coils, are used to change the direction of incident electron beam.

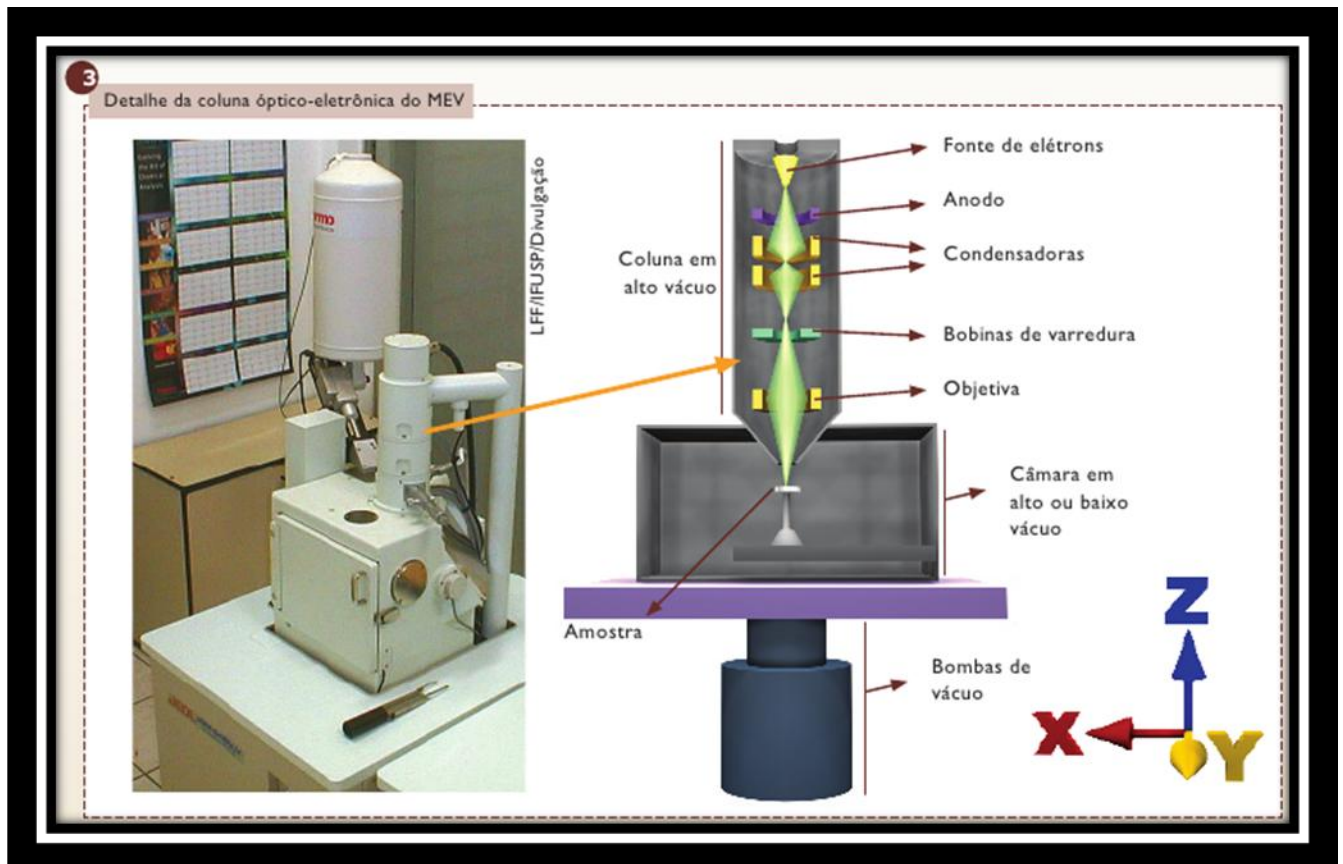


Fig. 2.2: Transmission Electron Microscope [25].

2.2.3 THERMOGRAVIMETRIC ANALYSIS AND DIFFERENTIAL SCANNING CALORIMETRY

In thermogravimetric analysis, mass of sample is recorded as a function of temperature. This analysis is very useful to study the thermal stability of sample [26]. In differential scanning calorimetry, the difference in the amount of heat required for increasing the temperature of sample and a reference is measured as a function of temperature [27]. This analysis is used to obtain melting point, enthalpy, specific heat etc.

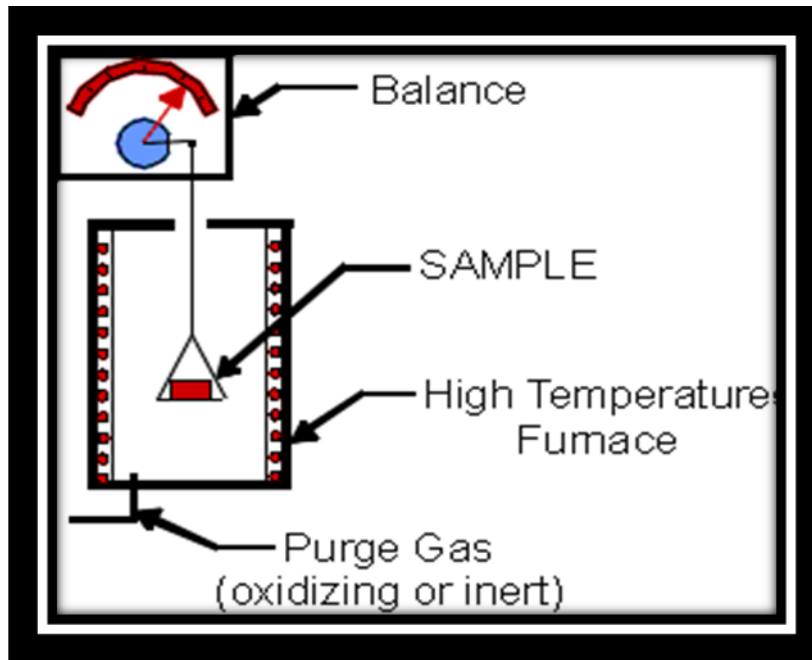


Fig. 2.3: Thermogravimetric analyzer [28].

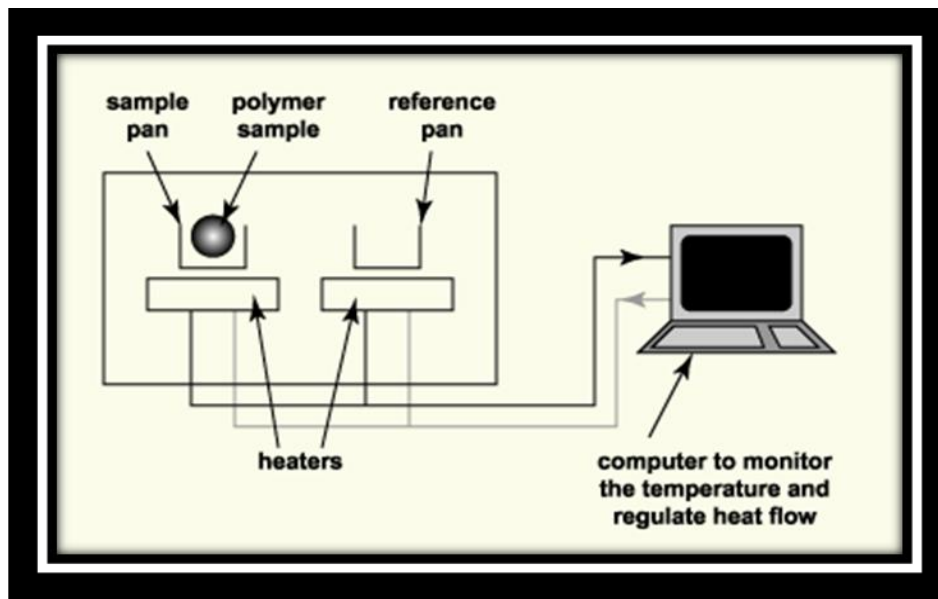


Fig. 2.4: Differential scanning calorimeter [29].

2.2.4 VIBRATING SAMPLE MAGNETOMETER

Vibrating sample magnetometer is used to measure magnetization of a given sample. This technique is based on the principle of Faraday's law of induction. It tells that a changing magnetic field induces an electrical field. By measuring the induced electric field, one can get an idea of the changing magnetic field. In this technique, an electromagnet is used to magnetize a sample. This magnetized sample is then allowed to vibrate along the vertical direction inside a pickup coil. The induced voltage across the coil is measured. This voltage is directly proportional to the magnetization of the sample. After a proper calibration, one can measure the magnetization of a given sample as a function of applied magnetic field and temperature [30].

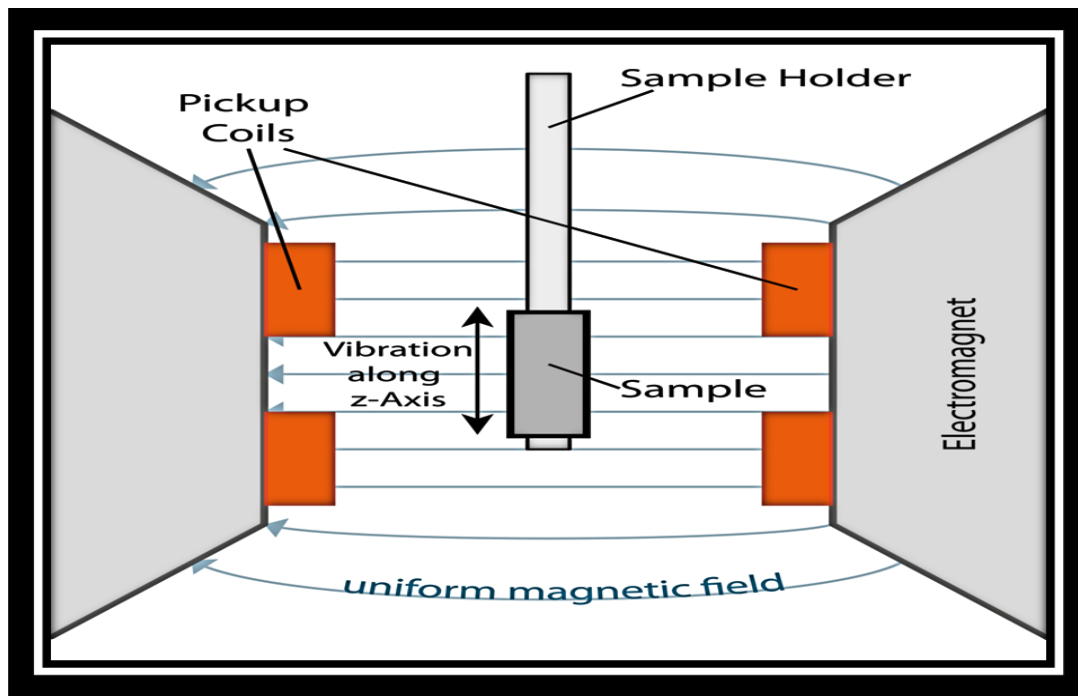


Fig. 2.5: Vibrating Sample Magnetometer [31].

CHAPTER 3

RESULTS AND DISCUSSIONS

3.1 STRUCTURAL CHARACTERIZATION

The structural characterization of synthesized undoped and Mo doped samples of ferrihydrite nanoparticles are done by x-ray diffraction and transmission electron microscopy. Room temperature x-ray diffraction patterns of samples are shown in Figures 3.1 and 3.2. From these figures it is clear that both samples are two lines ferrihydrite [17]. The diffraction peaks are also found to be broad. It indicates that the samples are nanocrystalline. The average crystallite size t is calculated by the modified Scherrer formula [32]

$$t = \frac{0.9\lambda}{\cos \theta_B (B_m - B_s)}$$

where λ is the wavelength of the x-ray used, θ_B is the Bragg's angle, B_m is the full width at half-maximum (FWHM) of a peak and B_s is the FWHM of the peak of a standard sample. The average crystalline sizes, using the modified Scherrer formula, for both samples turn out to be about 2 nm.

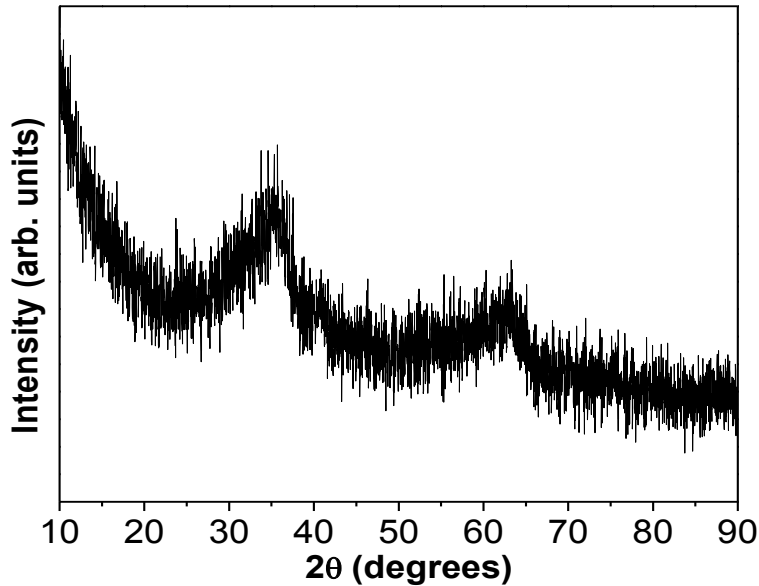


Fig. 3.1: X-ray diffraction pattern of undoped ferrihydrite nanoparticles.

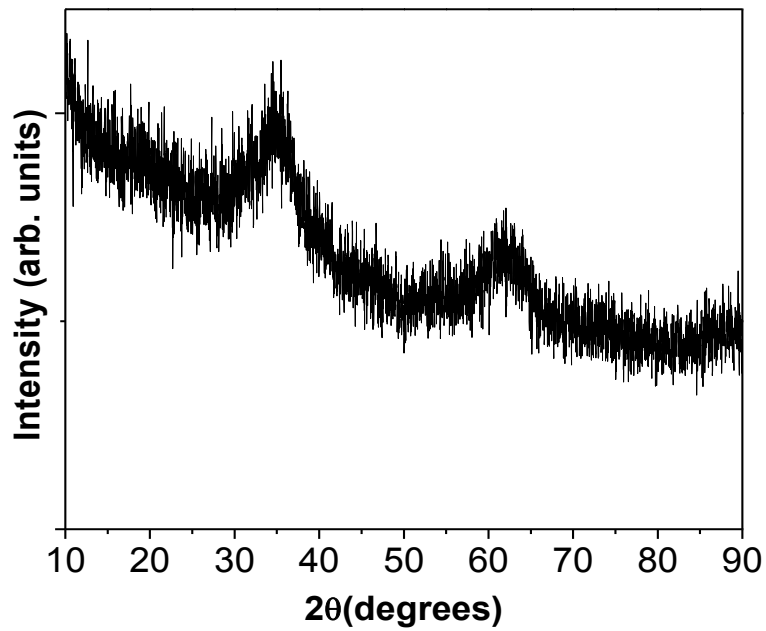


Fig. 3.2: X-ray diffraction pattern of Mo doped ferrihydrite nanoparticles.

Figures 3.3 and 3.4 show transmission electron micrographs of undoped and Mo doped samples. Clearly, the particles are of arbitrary shapes and sizes. The mean particle sizes are about 2 nm. The mean particle size determined by transmission electron micrograph is noted to be close to the average crystallite size determined by the x-ray diffraction using the modified Scherrer formula. It indicates that on an average each particle is a single crystallite.

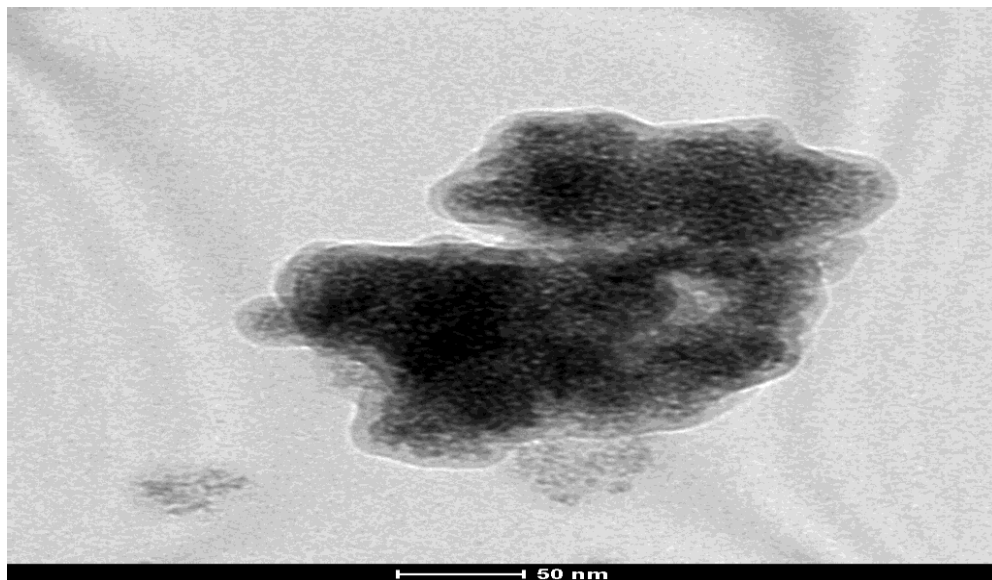


Fig. 3.3: TEM micrograph of undoped ferrihydrite nanoparticles.

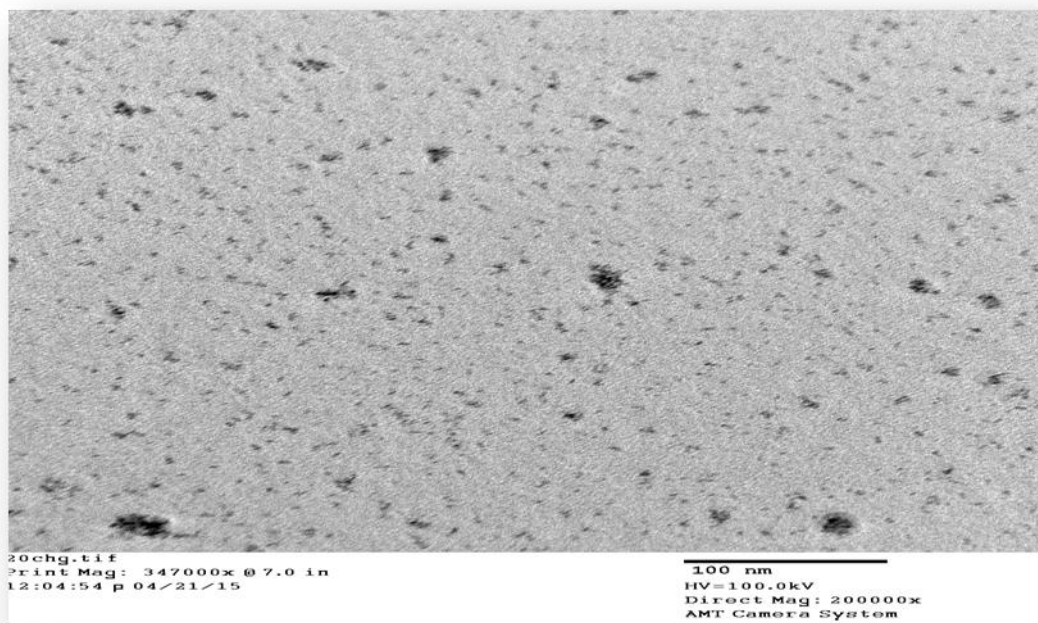


Fig. 3.4: TEM micrograph of Mo doped ferrihydrite nanoparticles.

3.2 THERMAL ANALYSIS

Synthesized samples are characterized by thermogravimetric analyzer and differential scanning calorimeter to study the stability of samples at higher temperatures. Details of these are shown in Figures 3.5 and 3.6. These figures show that the mass of sample decreases with increasing temperature and becomes almost constant at about 400 °C. In DSC curve, endothermic and exothermic peaks are observed near to 80 and 400 °C. At higher temperatures the samples are found to decompose into iron oxide.

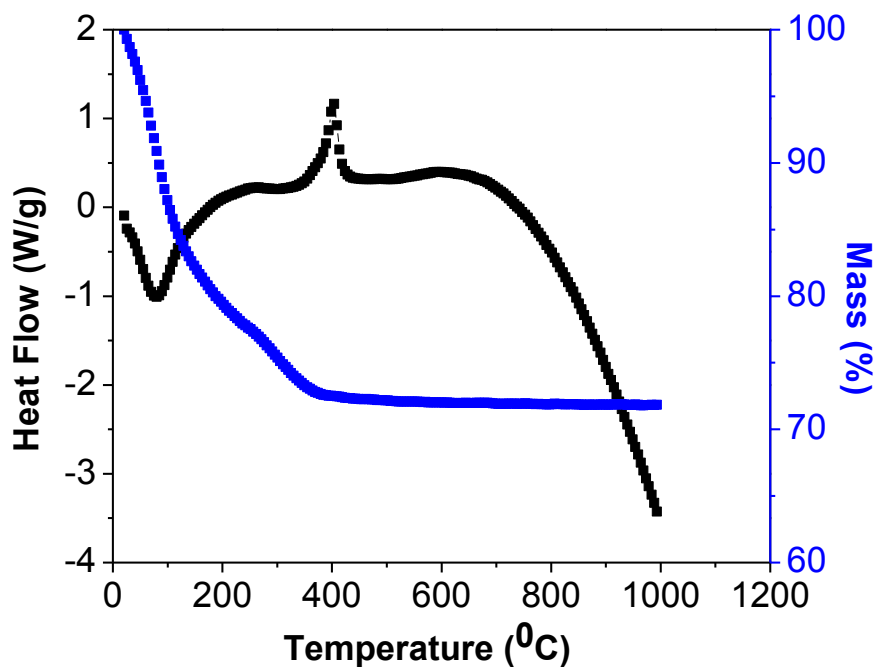


Fig. 3.5: TGA-DSC curves for undoped ferrihydrite nanoparticles.

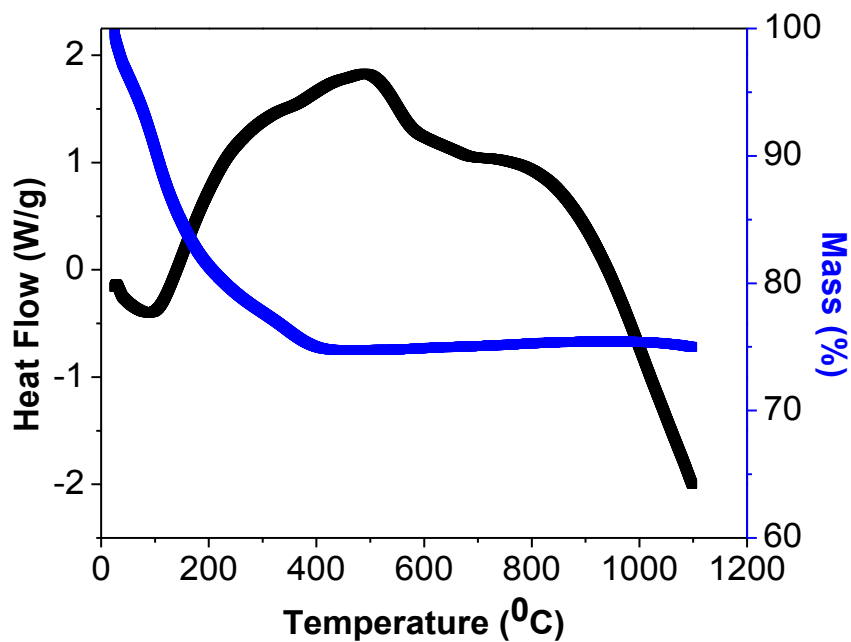


Fig. 3.6: TGA-DSC curves for Mo doped ferrihydrite nanoparticles.

3.3 MAGNETIZATION

Magnetization of undoped and Mo doped ferrihydrite nanoparticles are measured as a function of applied magnetic field at room temperature. These measurements are shown in Figure 3.7. This figure shows that there is no hysteresis in the magnetization as a function of magnetic field curve. The magnetization of the sample increases with increasing magnetic field linearly. From these measurements it is clear that both samples are antiferromagnetic at room temperature. The magnetization of Mo doped sample is found to be lower than that of undoped sample.

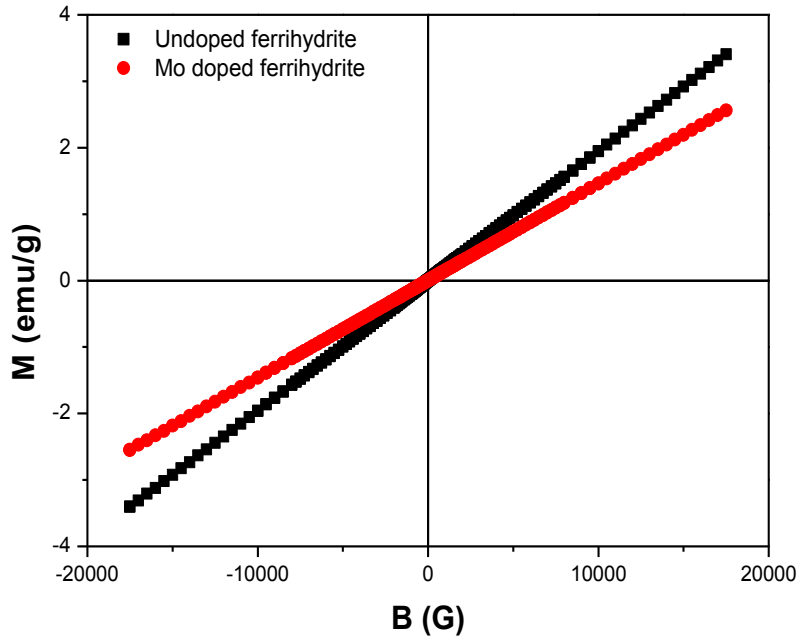


Fig. 3.7: M-B loop for undoped and Mo doped ferrihydrite nanoparticles at room temperature.

CHAPTER 4

CONCLUSION

Undoped and Mo doped ferrihydrite nanoparticles are synthesized by a chemical route. The average crystallite and particle sizes are found to be about 2 nm for both samples. Samples are found to be antiferromagnetic at room temperature. The magnetization of doped sample is found to be lower than that of undoped sample.

References

1. M. A. Willard, L. K. Kurihara, E. E. Carpenter, S. Calvin and V. G. Harris, in *Encyclopedia of Nanoscience and Nanotechnology*, Vol. 1, H. S. Nalwa (Ed.), p. 815, American Scientific Publishers, Stevenson Ranch, CA (2004).
2. P. Tartaj, in *Encyclopedia of Nanoscience and Nanotechnology*, Vol. 1, H. S. Nalwa (Ed.), p. 177, American Scientific Publishers, Stevenson Ranch, CA (2004).
3. Q. A. Pankhurst, J. Connolly, S. K. Jones and J. Dobson, *J. Phys. D: Appl. Phys.* **36**, 167 (2003).
4. C. Kittel, *Introduction to Solid State Physics*, John Wiley and Sons, Inc., Seventh Edition, 1996.
5. Ashcroft N. W. and Mermin N. D., *Solid State Physics*, Harcourt Asia Pvt. Ltd., 1976.
6. A. J. Dekker, *Solid State Physics*, Macmillan India Limited, 1996.
7. V. Raghavan, *Materials Science and Engineering*, PHI Learning Private Limited, Fifth Edition, 2010.
8. W. F. Smith and J. Hashemi, *Foundation of Materials Science and Engineering*, McGraw Hill International Edition, Fourth Edition, 2006.
9. http://www.vectorsite.net/tpqm_04.html.
10. http://en.wikipedia.org/wiki/File:Antiferromagnetic_ordering.svg.
11. http://www.tf.uni-kiel.de/matwis/ammat/elmat_en/kap_4/backbone/r4_1_3.html.
12. I. S. Jacobs and C. P. Bean, in *Magnetism*, G. T. Rado and H. Suhl (Eds.), Vol. III, p. 271, Academic Press Inc., New York, 1963.
13. V.A. Drits, B.A. Sakharov, A.L. Salyn and A. Manceau, *Clay Minerals* **28**,185 (1993).
14. J. Zhao, F. E. Huggins, Z. Feng and G. P. Huffman, *Clay and Clay Minerals* **42**, 737 (1994).
15. J. L. Jambor and J. E. Dutrizac, *Chem. Rev.* **98**, 2549 (1998).
16. M. S. Seehra, V. S. Babu and A. Manivannan, *Physical Review B* **61**, 3513 (2000).
17. A. Punnoose, T. Phanthavady, M. S. Seehra, N. Shah, G. P. Huffman, *Phys. Rev. B* **69** 54425 (2004).
18. F. M. Michel, L. Ehm, G. Liu, W. Q. Han, S. M. Antao, P. J. Chupas, P. L. Lee, K. Knorr, H. Eulert, J. Kim, C. P. Grey, A. J. Celestian, O J. Gillow, M. A. A. Schoonen, D. R. Strongin and J. B. Parise, *Chem. Mater.* **19**, 1489 (2007).

19. D. Carta, M.F. Casula, A. Corrias , A. Falqui, G. Navarra and G. Pinna, *Materials Chemistry and Physics* **113**, 349 (2009).
20. L. Dyer, P. D. Fawell, O.M.G. Newmanc and W. R. Richmond, *Journal of Colloid and Interface Science* **348**, 65 (2010).
21. S .Das, M . Jimhendry and J. E. Dughan, *Environ. Sci. Technol.* **45**, 268 (2011).
22. C. Rani and S.D. Tiwari, *J of Magn. Magn. Matter.* **385**, 272 (2015).
23. [http://www.asdlib.org/online Articles/ecourseware/BullenXRD/Learning Activity Diffraction \(BraggsLaw.pdf\)](http://www.asdlib.org/online%20Articles/ecourseware/BullenXRD/Learning%20Activity%20Diffraction%20(BraggsLaw.pdf)).
24. http://en.wikipedia.org/wiki/Transmission_electron_microscopy.
25. <https://www.google.co.in/search?q=IMAGES+OF+TEM&rlz>.
26. C. J. Keattch and D. Dollimore, *An Introduction to Thermogravimetry*, Heyden, London, 2nd edn, 1975.
27. J. Sestak, *Thermophysical Properties of Solids*, Academia, Prague, 1984.
28. http://radchem.nevada.edu/classes/chem455/lecture_22__thermal_methods.htm.
29. http://www.ami.ac.uk/courses/topics/0140_pl/index.html
30. S. Foner, *The Review of Scientific Instruments* **30**, 548 (1959).
31. <https://www.google.co.in/search?q=IMAGES+OF+VSM>.
32. B. D. Cullity, *Elements of X-Ray Diffraction*, Adiison-Wesley Publishing Company, Inc., 1956.